CHAPTER II: THE SUN AND SUNLIGHT

Introduction

Any discussion of solar energy and solar (photovoltaic) cells should begin with an examination of the energy source, the sun. Our sun is a dG2 star, classified as a yellow dwarf of the fifth magnitude. The sun has a mass of approximately 10^{24} tons, a diameter of 865,000 miles, and radiates energy at a rate of some 3.8×10^{20} megawatts. Present theories predict that this output will continue, essentially unchanged, for several billion years. It is necessary to say essentially, because the sun's energy output may fluctuate by a few percent from time to time. For our purposes we will consider the solar energy output to be a constant.

Between the sun and the earth there exists a hard vacuum and a distance which varies from 92 to 95 million miles. This distance variation implies, using the inverse square law, that the light energy reaching the earth in June (when the earth is at its maximum distance from the sun) is approximately 94% of the light energy reaching the earth in December [1]. In this work, we will follow the common practice of assigning an average value to the light energy density available to a collector positioned just outside the earth's atmosphere. This quantity is known as the solar constant and has been measured variously as lying between 0.1338 and 0.1418 W/cm^2 [2]. Four our purposes, we will take for the solar constant [3]:

Solar Constant = 0.1353 W/cm^2. (II.2)

This power density is available, on the sunlit side of the earth, 24 hours a day, each day of the year, yielding an annual energy flux to the earth of 1,186 kwh/cm^2.

Once the sunlight has reached the earth's atmosphere a number of additional effects play a part. Those effects resulting from weather, and photon absorption by water vapor, ozone, and other atmospheric

constituents will be considered in detail later in this chapter. They have the general overall effect of reducing the energy density in sunlight at the earth's surface. Atmospheric effects are at a minimum on a dry, cloudless day with the sun directly overhead (and at the zenith). Under these conditions (known collectively as air-mass-one or AM1) the power flux in sunlight at the earth's surface is [2, 4]:

$$\text{AM1 power flux} = 0.107 \text{ W/cm}^2. \qquad \text{(II.2)}$$

Two other factors influencing the availability of solar energy are geometric in nature. The first we have already considered, in part. The earth rotates on its axis with a period of approximately 24 hours, hence sunlight is available for only an average of 12 hours a day. Next, the earth's axis of rotation is tilted approximately 23.5° to the normal of its plane of revolution about the sun. Together, these two effects act to produce a shift in the number of hours of daylight and a geometrical situation in which the sun is almost never directly overhead, thereby enhancing light losses due to various atmospheric phenomena.

Sunlight

The observed solar light output (spectrum) is not constant with respect to wavelength or to time. Time variations depend on solar flares, sunspot activity, and other phenomena. Overall, the variation in solar output with wavelength corresponds quite closely to that expected of a 5,800 °K black-body radiator. However, there are departures due to Fraunhofer absorption lines and a number of emission lines from the solar corona and elsewhere close to the surface of the sun [5, 6]. For our purposes, the solar spectral irradiance, defined as the power density per unit wavelength in sunlight, may be presented as a time and wavelength smoothed envelope. This is done in Figure II.1 [4-11]. The outer curve depicts the solar spectral irradiance above the earth's atmosphere; the condition known as air-mass-zero (AMO). The inner curve in Figure II.1 is the solar spectral irradiance at sea level with the sun at the zenith on a clear, dry day--the air-mass-one condition. Note that the inner curve shows the effects of ozone on the ultraviolet portion of the spectrum and the effects of water vapor, smog, carbon dioxide and other atmospheric gases and pollutants on the long wavelength portions of the spectrum.

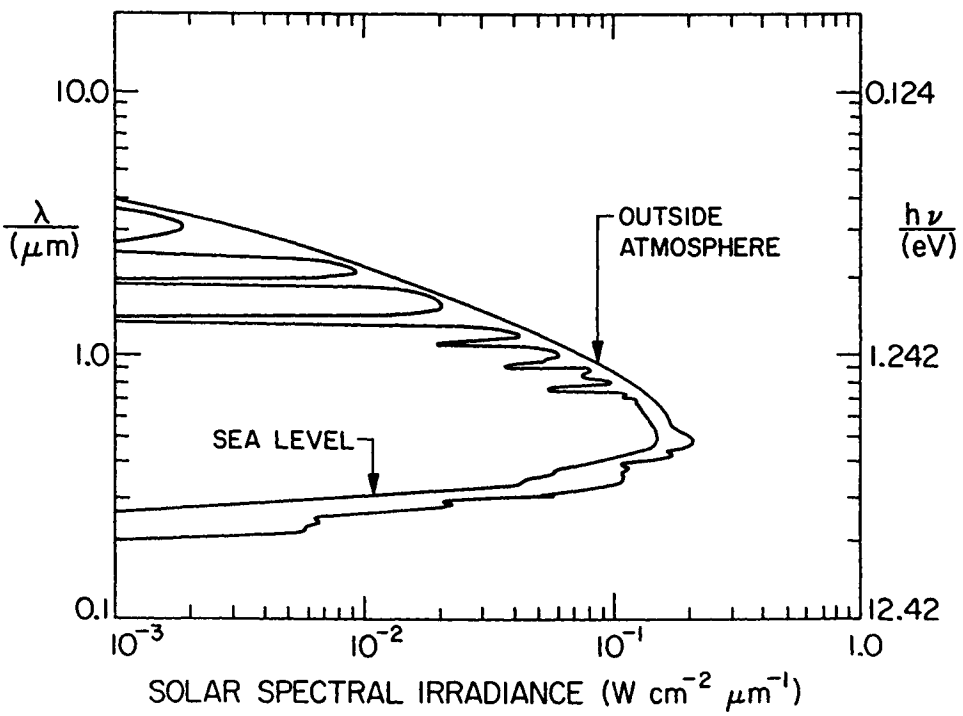

Figure II.1. The solar spectral irradiance as a function of wavelength and photon energy, with atmospheric location as a parameter.

As indicated earlier, the air-mass-zero condition corresponds to a solar power flux density of 0.1353 watts per square centimeter and a potential of 24 hours of sunlight each day. The air-mass-one condition corresponds to a maximum power flux density of 0.107 watts per square centimeter and a potential average of approximately 12 hours a day of sunlight.

Under air-mass-zero (AMO) conditions the annual energy flux density is 1.188 kwh/cm^2, but under air-mass-one (AM1) conditions the maximum energy density is reduced to 0.469 kwh/cm^2 per year. In actuality, the earth's rotation, combined with weather effects, reduces this value still further. It is this difference in potential energy density that prompts discussion of energy collection stations in orbit about the earth. There are, naturally a number of problems to be considered in the construction of extra-terrestrial energy stations. Not the least of these are the effort involved in boosting the station components to orbit, the construction of the station and the maintenance of the station. (The potential energy difference between the earth's surface and a space station orbiting over a fixed point on the earth's surface is 5.3 x 10^8 joules per kilogram of mass. To supply a net of 4 Q of energy to the earth, an orbiting solar energy collection/conversion facility, with a 20% operating efficiency, must have an area of approximately a million square kilometers--implying a considerable mass.) A potential ecological problem with space power lies in the fact that, as a result of the energy collection, a net input of additional energy is made to the earth (in the case of the preceding example, slightly less than 0.1% of the naturally occurring solar energy flux). Whether this additional energy would have any environmental effect, we cannot answer at present. The economics and technical design aspects of solar space stations are discussed in the literature [12]. We will not go into additional detail here. However, in connection with the question of space- or surface-based solar energy converter/collectors, note that more energy exists in the ultraviolet under AMO conditions. This implies that the design of a photovoltaic (solar) cell for AMO conditions must be different from the design of a solar cell for AM1 conditions. This topic will be discussed in a later chapter.

In Figure II.1 there are two ordinate scales. In one, the wavelength of the solar radiation is portrayed. However, in working with solar cells it is frequently more convenient to discuss the effects in terms of the energies of the individual photons--thus leading to the second scale. The conversion from one scale to the other is easily made using the following:

Photon energy (in ev) = $1.243/\lambda$(in μm) (II.3)

The basic quantity is, of course, the energy available in sunlight. Integrating over Figure II.1, we arrive at the wavelength versus energy distribution of Table II.1. Note that a significant fraction of the solar spectral irradiance lies at wavelengths greater than 1.15 μm. This region of the solar spectrum is often termed the far infrared, as opposed to the near infrared (which lies between 0.7 and 1.15 μm). In later chapters it will be demonstrated that this far infrared region is not available to solar cells as an energy source. This is a major limitation on the efficiency of energy producing photovoltaic devices.

Table II.1

Solar spectral irradiance under air-mass-zero and air-mass-one conditions as a function of wavelength

Wavelength (μm)	Photon Energy (ev)	Solar Spectral Irradiance (milliwatts/cm^2)	
		AMO	AM1
∞ - 1.15	0.00 - 1.08	31.77	25.24
1.15 - 1.00	1.09 - 1.24	9.51	8.41
1.00 - 0.90	1.25 - 1.38	8.29	6.02
0.90 - 0.80	1.39 - 1.55	9.93	8.35
0.80 - 0.70	1.56 - 1.78	12.37	8.05
0.70 - 0.60	1.79 - 2.07	15.15	13.25
0.60 - 0.50	2.08 - 2.49	17.70	14.30
0.50 - 0.40	2.50 - 3.11	18.77	15.10
0.40 - 0.30	3.12 - 4.14	10.17	7.91
0.30 - 0.20	4.15 - 6.22	1.63	0.37
0.20 - 0.00	6.23 - ∞	00.01	00.00
	Total	135.30	107.00

We will return to the data of this table in later chapters as the selection of semiconducting materials for and the design of solar cells is considered in detail. Let us now turn our attention to the effects of geometrical situations on solar energy.

Geometrical Effects

Perhaps the simplest geometrical effect is that due to altitude. Simply moving up a tall mountain reduces the atmospheric losses, a fact evidenced by the darker sky in regions of high elevation. Observations by Laue [13] indicate an increase of approximately 18% in solar power flux density for an increase in altitude from sea level to three kilometers, when the sun is at the zenith. This enhancement in solar energy, while significant in the sense that there are many areas of sun and high altitude on our planet, will not be considered in the rest of this work. Thus, what follows may be considered to be a conservative estimate of the available solar energy, as all locations are treated as being at sea level.

As discussed in the introduction to this chapter, the earth's rotation and axial tilt introduce a variation in the length of day, both as a function of the time of year and or latitude. While this has no effect on an orbiting solar energy collection/conversion system, it strongly affects collectors on the earth's surface.

The solar input power under air-mass-one is 1.07 kw/m^2. This condition implies a vertical orientation for the sun and solar collectors that are at right angles to the direction to the sun. The earth rotates with an axis angle of 23.5° and a period of approximately 24 hours. Hence, the sun is seldom, if ever, directly overhead (as depicted in Figure II.2). Should the sun make an angle, ψ, with the normal of a detector lying flat upon the ground (again, as shown in Figure II.2), the available solar power density, P, is given by:

$$\text{Solar Power Density} = P = \alpha(\psi)\cos\{\psi\}, \qquad \text{(II.4)}$$

where $\alpha(o)$ = 1.07 kw/m^2 under AM1 conditions. In general, the factor alpha is a function of the angle, ψ. As light traverses the atmosphere, it is partially absorbed and partially scattered by the gases in the air and any contaminants in the atmosphere. The greater the angle, ψ, the further the sun is from the normal and the greater the thickness of atmosphere which must be traversed and the more photons are scattered and/or absorbed. Thus, the value of alpha decreases with increasing psi. Table II.2 lists values of alpha as a function of the angle, psi, [14].

The angle, ψ, varies daily from sunrise to sunset, and also on a monthly basis, as the sun angle at noon (noon being defined as that time of day when the sun angle, ψ, is at a minimum) varies from L - 23.5° in

June to L + 23.5° in December, where L, the latitude is in degrees*.

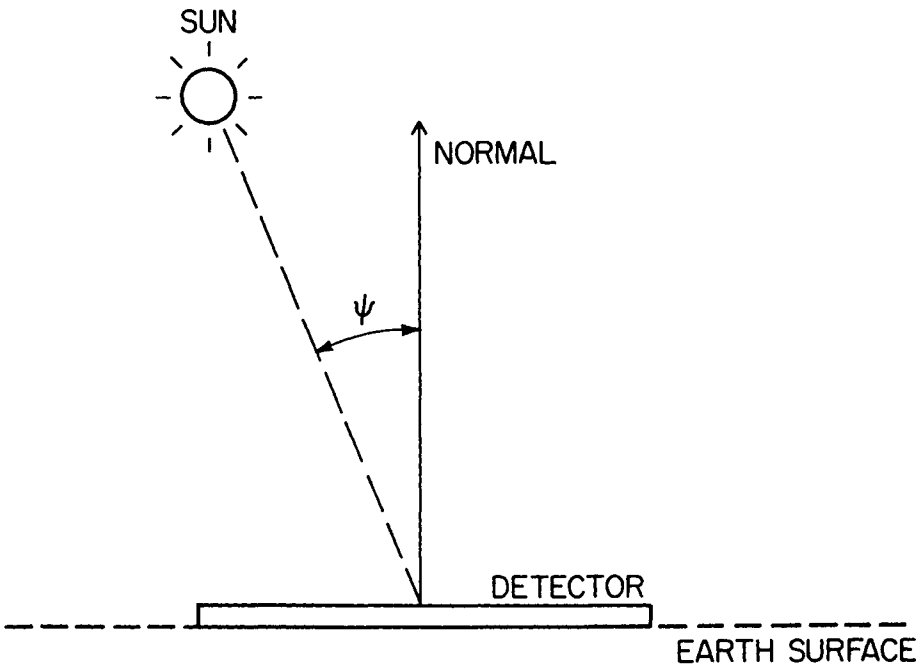

Figure II.2. Sun and detector orientations for typical daylight conditions [11].

Table II.2

Atmospheric effects on solar power input as a function of the solar angle, ψ (see Figure II.2)

ψ (°)	0	10	20	30	40	45	50	55
α(kw/m^2)	1.07	1.06	1.05	1.03	0.993	0.968	0.939	0.903
ψ (°)	60	70	75	80	85	87	88	
α(kw/m^2)	0.855	0.717	0.603	0.451	0.233	0.142	0.095	

* This assumes a Northern Hemisphere location for the solar collector. In the Southern Hemisphere, the signs should be reversed.

It is possible to eliminate the geometric portion, $\cos\{\psi\}$, of Equation II.4 by tilting the detector until the sun is aligned with the collector normal. Figure II.3 indicates the angular positions for such a tiltable collector (not yet perfectly aligned) when positioned in the Northern Hemisphere. However, such an action will not reduce the length of the atmospheric path, and, hence, the effect on $\alpha(\psi)$.

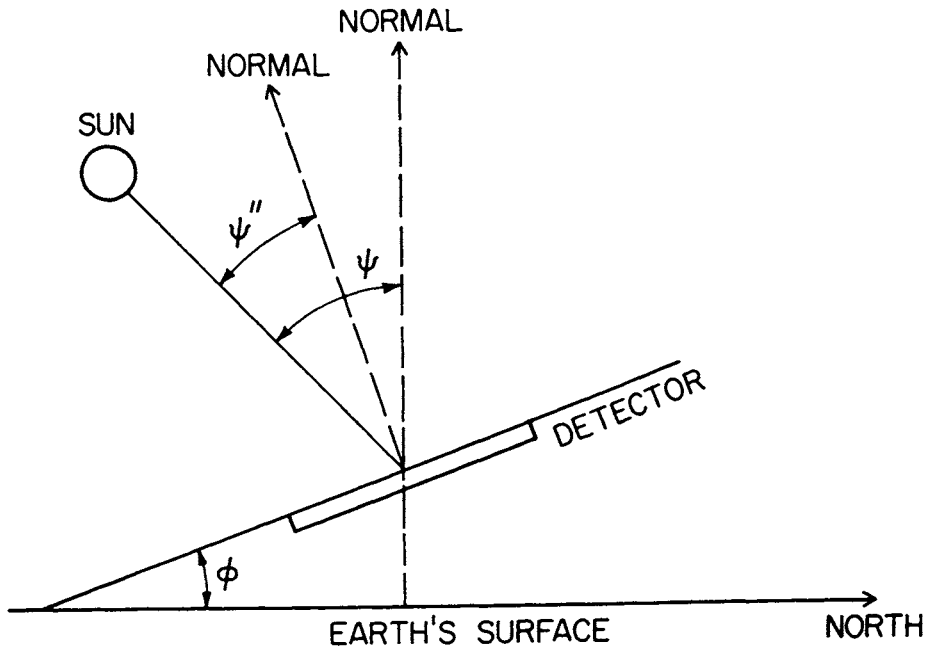

Figure II.3. Detector, sun and earth orientations for a tiltable solar detector/collector [11].

The average year is 365 and a fraction days long, during which time the sun traverses approximately 47° from north to south and back again. Therefore, the change in solar angle measured on a north-to-south basis is approximately eight degrees per month, a relatively small number. Each day, however, the sun rises in the east and sets in the west, covering about 180 degrees of arc in an average period of 12 hours. In computing the total solar insolation (TSI), defined as the energy received each day directly from the sun, a reasonable value can be obtained using the following expression:

$$TSI = 2 \int^{D/2} \alpha(\psi)\cos\{\psi''\}dt, \qquad (II.5)$$

where D is the amount of daylight for a given day, α is determined by computing the solar angle ψ (see Figure II.3) and using Table II.2, and ψ'' is defined in Figure II.3.

There are several solar energy collector configurations of interest. (A) We can consider the collector to be a device lying, unmoving, flat upon the ground. In this case, the angle of the collector with respect to the ground, ϕ in Figure II.3, is zero. (B) The collector can be mounted upon some mechanism that insures that the collector is always pointed at the sun with the angle, ψ'', in Figure II.3 zero at all times. (C) A collector can be mounted upon the ground, unmoving, but at some fixed angle, ϕ, to the horizontal. This angle will be southward facing in the Northern Hemisphere, as shown in Figure II.3 and will be, clearly, northward facing in the Southern Hemisphere. A final class of collector, (D), is fixed at some angle, ϕ, in the north-to-south direction, but is capable of following the sun in its east-to-west motion*.

For a horizontally mounted, unmoving solar energy collector:

$$\tan^2(\psi) = \tan^2(\psi') + \tan^2(\theta), \qquad (II.6)$$

where ψ' is the average north-south angle, for a given day, between the sun and the zenith, and θ is the east-west angle between the sun and the surface normal as the sun traverses the sky from sunrise to sunset. As a function of time, we may write for θ:

$$\theta = (1 - 2t/D)\pi/2 \text{ for } 0 < t \leq D/2, \qquad (II.7)$$

where t is the time (a value of zero corresponds to sunrise).

For an unmoving, but angled collector:

$$\tan^2(\psi'') = \tan^2(\psi' - \phi) + \tan^2(\theta). \qquad (II.8)$$

* This type of collector is known as a polar-axis tracking collector or single-axis polar tracking collector, as opposed to type B which is a two-axis tracking collector.

For a collector that tracks the sun only from east-to-west (a single-axis collector):

$$\psi'' = \psi - \phi. \tag{II.9}$$

For a full (two-axis) tracking collector:

$$\psi'' = 0. \tag{II.10}$$

In Figure II.4 the solar insolation (TSI), in kwh/m^2, per year is presented for latitudes from zero (the equator) to 70° with collector orientation (the angle ϕ in Figure II.3) and tracking mode as parameters. As before, the No Tracking mode implies a collector which is fixed at some north-to-south angle; East-West Tracking implies a mechanism that moves the collector only in the east-to-west direction, while the north-to-south angle is fixed at the given angle (this omits corrections for changes in the seasonal north-to-south solar orientation); and Ideal Tracking signifies a two-axis tracking mode that maintains the collector normal pointed at the sun at all times that the sun is above the horizon.

Study of Figure II.4 shows that the use of an east-west tracking mode system yields an insolation which is close to the maximum value provided by two-axis tracking whenever the optimum north-to-south angle is selected. This optimum angle is clearly a function of the latitude. It is also evident from Figure II.4 that fixed collectors are much less effective as energy collectors than either the single-axis or two-axis tracking collectors.

Later in this work we will encounter other and even more powerful arguments for the use of tracking mechanisms. However, the enhanced efficiency evidenced in Figure II.4 is more than sufficient to make serious consideration of solar collectors with tracking mechanisms attractive.

In Figure II.5, the optimum collector angle, ϕ, and the accompanying maximum insolation are plotted as a function of latitude, with the tracking mode as a parameter. This figure serves to emphasize, once more, the desirability of some form of tracking. Note that the optimum collector angle (on a north-to-south basis) for east-west tracking systems is approximately equal to the latitude.

Figures II.4 and II.5 do not convey the total picture. For some locations and some climates, the maximization of insolation over an entire year may not be as desirable as the maximization of insolation for a

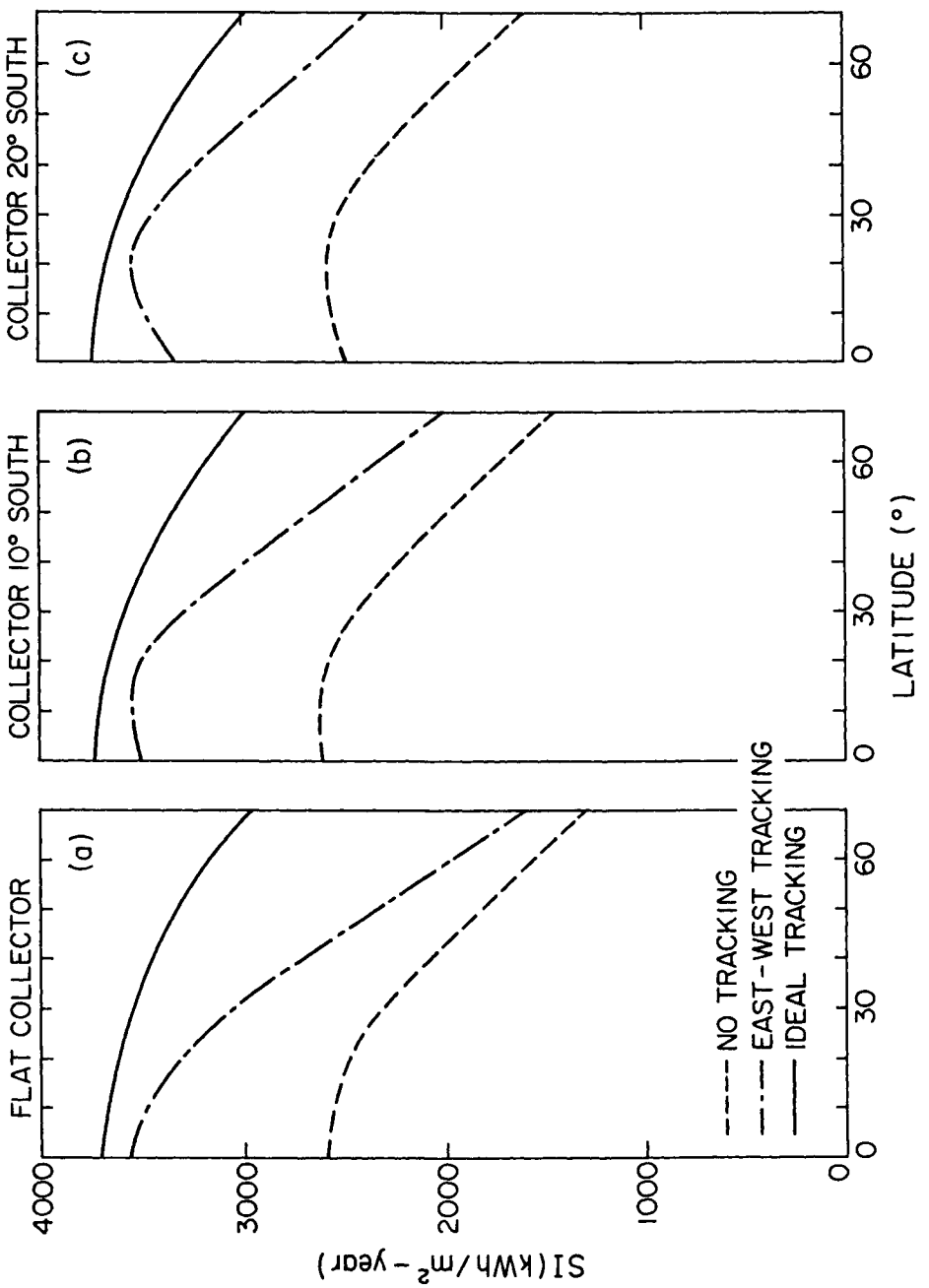

Figure II.4 a,b,c. Solar input (insolation) per square meter per year at the earth's surface as a function of latitude and collector tilt, with the tracking mode as a parameter [11].

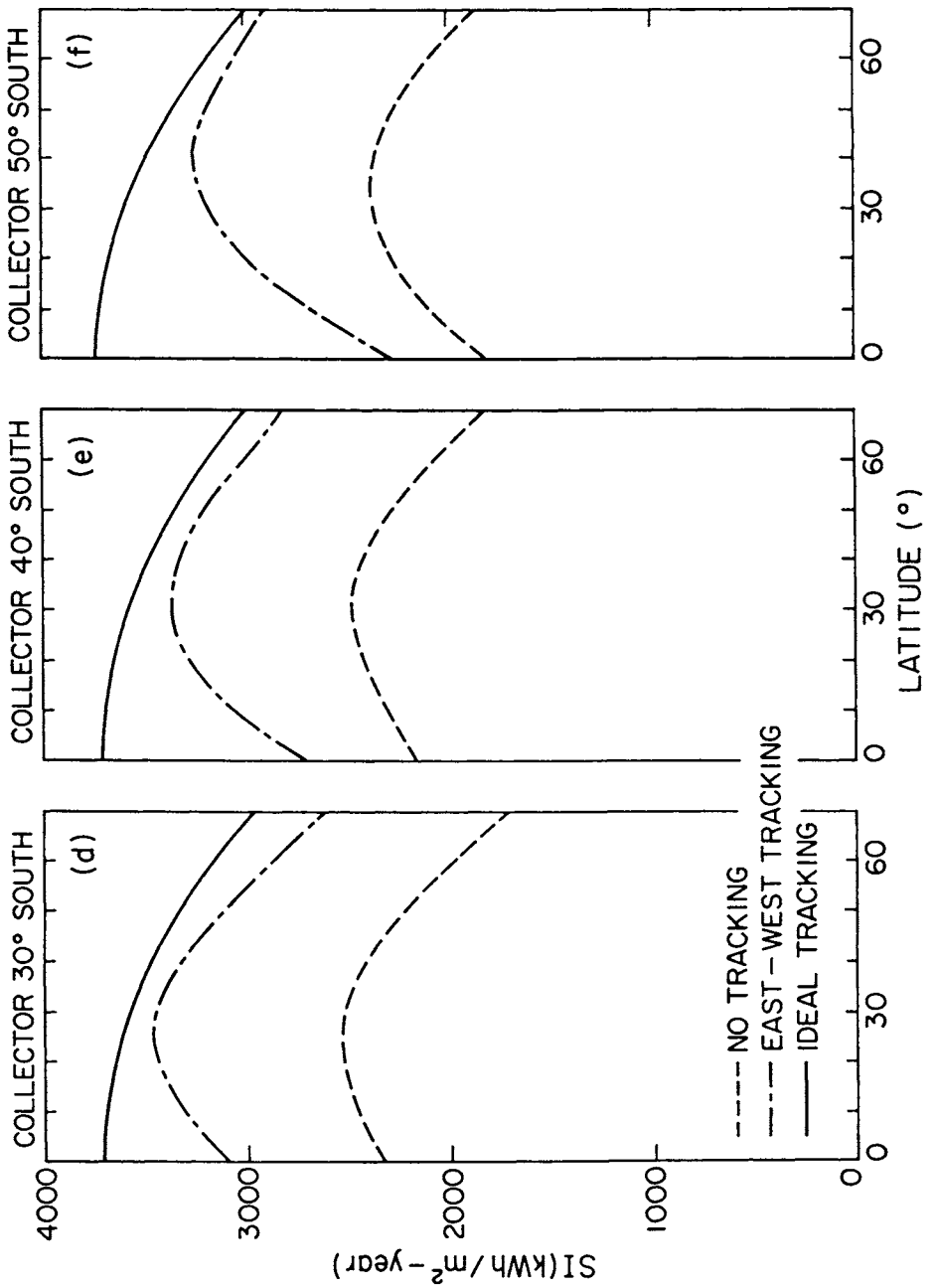

Figure II.4 d,e,f. Solar input (insolation) per square meter per year at the earth's surface as a function of latitude and collector tilt, with the tracking mode as a parameter [11].

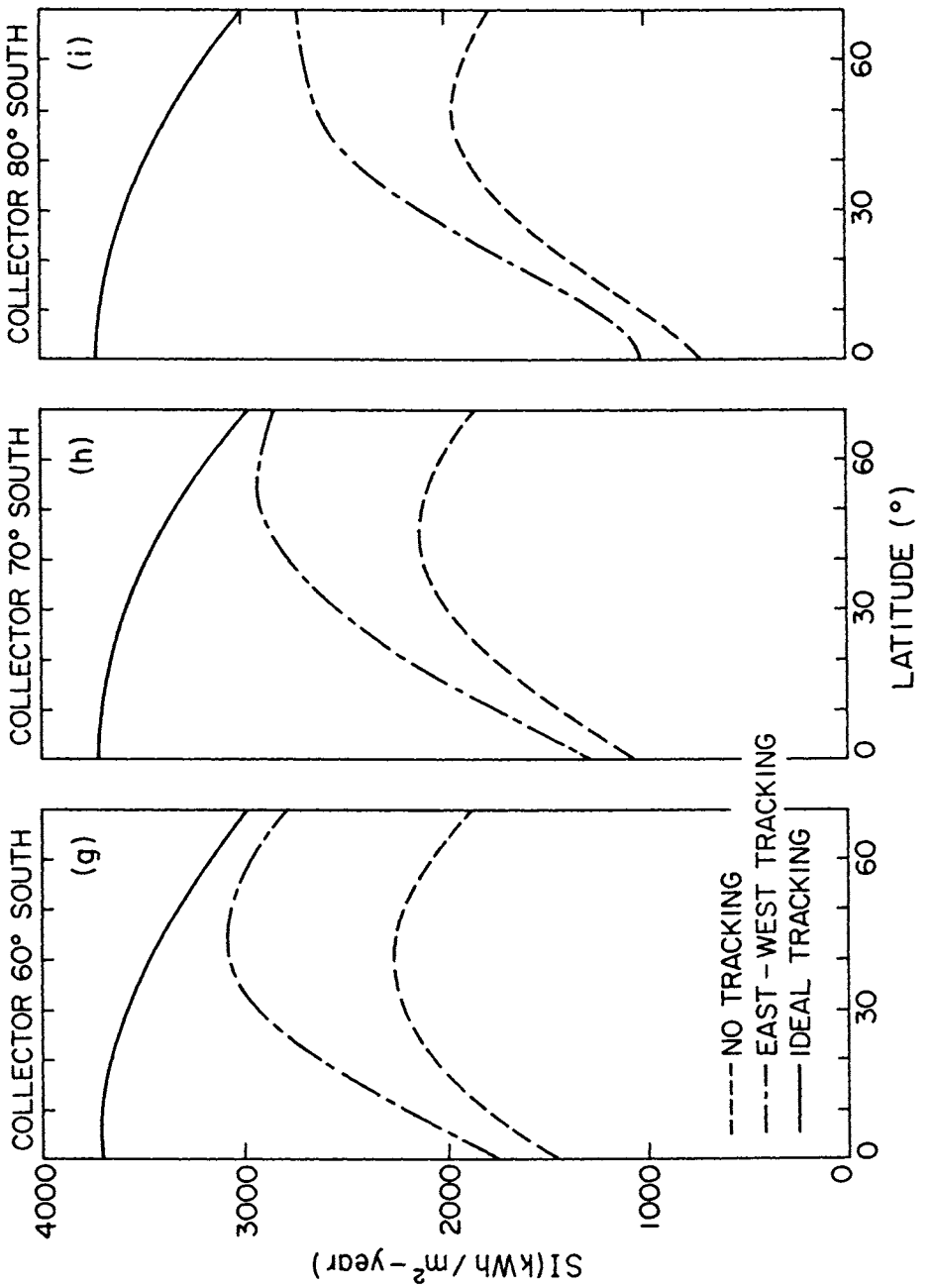

Figure II.4 g,h,i. Solar input (insolation) per square meter per year at the earth's surface as a function of latitude and collector tilt, with tracking mode as a parameter [11].

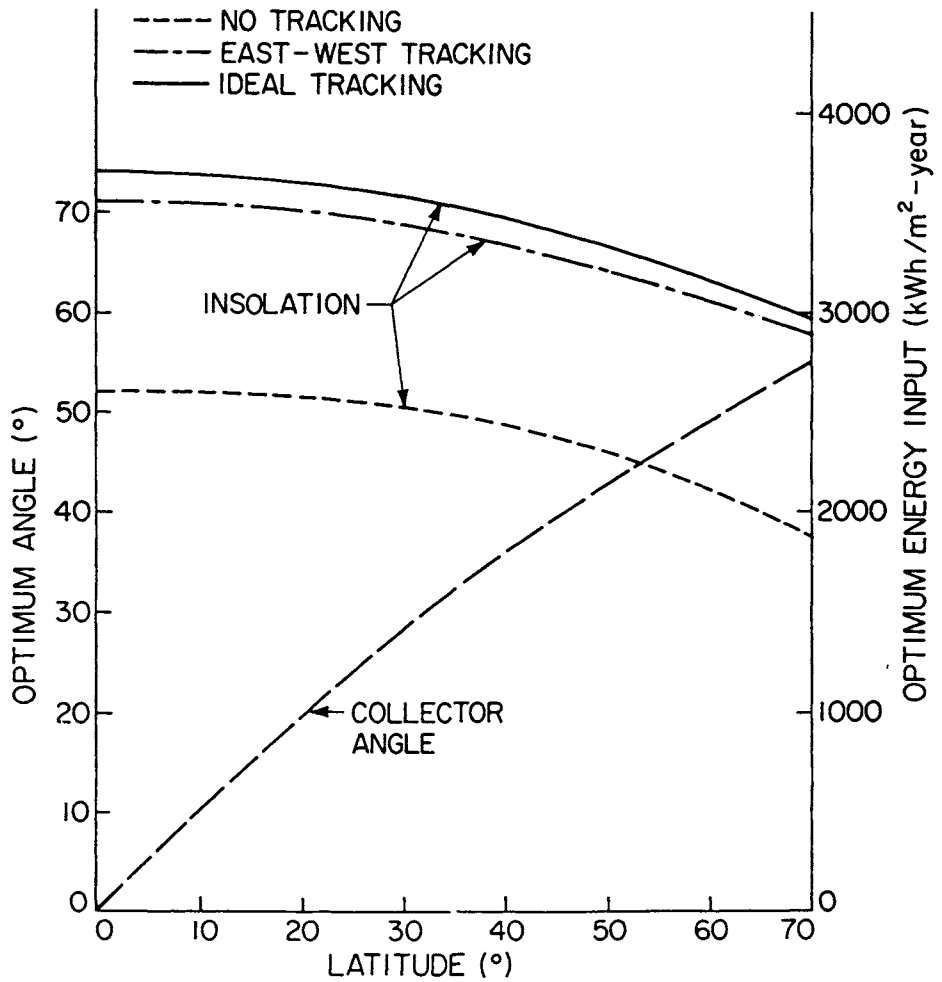

Figure II.5. The optimum collector angle and maximum energy input as a function of latitude for No Tracking (fixed), East-West Tracking (single-axis) and Ideal (two-axis) Tracking [11].

particular season, such as summer in Tucson, Arizona. Table II.3 presents the insolation, by season for the three tracking modes as a function of collector orientation angle, ϕ, with latitude as a parameter. Clearly, the collector orientation angle, ϕ, is important only for fixed position and single-axis tracking systems. For the purposes of Table II.3, winter is defined as that third of the year that has as its midpoint, the winter solstice; summer is defined as that third of the year that has as its midpoint, the summer solstice.

Table II.3

Seasonal available insolation (kwh/m^2) as a function of latitude and tracking mode with north-to-south tracker angle, ϕ, (in degrees), as a parameter

ϕ	0	10	20	30	40	50	60
			Latitude of zero degrees				
Winter							
--Two-axis	1220	1220	1220	1220	1220	1220	1220
--One-axis	1160	1210	1210	1200	1150	1050	930
--Fixed	850	880	890	880	850	800	730
Summer							
--Two-axis	1220	1220	1220	1220	1220	1220	1220
--One-axis	1160	1070	950	800	620	430	220
--Fixed	850	820	740	650	530	390	220
			Latitude of ten degrees				
Winter							
--Two-axis	1170	1170	1170	1170	1170	1170	1170
--One-axis	1020	1100	1150	1160	1150	1090	1000
--Fixed	770	810	840	850	840	810	760
Summer							
--Two-axis	1280	1280	1280	1280	1280	1280	1280
--One-axis	1260	1200	1110	990	830	650	440
--Fixed	920	890	840	770	680	550	400
			Latitude of twenty degrees				
Winter							
--Two-axis	1090	1090	1090	1090	1090	1090	1090
--One-axis	840	950	1030	1070	1080	1070	1020
--Fixed	650	710	760	780	790	780	750
Summer							
--Two-axis	1330	1330	1330	1330	1330	1330	1330
--One-axis	1320	1310	1280	1190	1060	880	680
--Fixed	970	960	930	870	800	700	570
			Latitude of thirty degrees				
Winter							
--Two-axis	990	990	990	990	990	990	990
--One-axis	650	770	860	940	980	980	980
--Fixed	520	590	640	680	700	710	700

Table II.3, continued

ϕ	0	10	20	30	40	50	60
Summer							
--Two-axis	1390	1390	1390	1390	1390	1390	1390
--One-axis	1360	1380	1370	1310	1200	1010	900
--Fixed	1000	1000	990	960	910	830	730
			Latitude of forty degrees				
Winter							
--Two-axis	850	850	850	850	850	850	850
--One-axis	430	550	660	740	830	840	840
--Fixed	360	440	500	550	580	600	600
Summer							
--Two-axis	1460	1460	1460	1460	1460	1460	1460
--One-axis	1370	1440	1450	1440	1380	1270	1130
--Fixed	1010	1040	1050	1040	1000	950	870
			Latitude of fifty degrees				
Winter							
--Two-axis	650	650	650	650	650	650	650
--One-axis	230	340	430	510	570	620	640
--Fixed	200	280	340	380	420	440	450
Summer							
--Two-axis	1540	1540	1540	1540	1540	1540	1540
--One-axis	1330	1450	1520	1520	1520	1450	1340
--Fixed	1010	1040	1070	1080	1070	1040	980
			Latitude of sixty degrees				
Winter							
--Two-axis	340	340	340	340	340	340	340
--One-axis	70	130	180	230	270	300	320
--Fixed	60	100	140	170	200	220	230
Summer							
--Two-axis	1710	1710	1710	1710	1710	1710	1710
--One-axis	1300	1470	1600	1680	1700	1680	1610
--Fixed	1010	1040	1080	1100	1130	1160	1120

Weather

There remains a major variant that must be considered in

determining the insolation available to any collector, the climate of the particular region in which the collector is operating.

This volume is concerned with solar (photovoltaic) cells. Such devices require direct solar radiation for efficient operation. Weather is a highly variable factor, both in the short and long term (15-20), so variable that we are forced to use statistical approaches and average values in order to assess its effects.

Consider, for example, Table II.4. In this table we present, for twenty cities, the maximum insolation obtainable by a two-axis tracking collector and, with statistically averaged weather effects included, the insolation available to a tracking collector and to a horizontally mounted unmoving solar collector. This last quantity is the amount of solar energy that is normally available at the earth's surface at any given location. The variation observable in Table II.4 explains the known datum that the polar regions are cold and the equatorial regions of the earth are hot!

Since weather data, particularly cloud cover, are extremely location dependent, any specific solar collector design must be based on local weather conditions. General pictures such as those furnished in Table II.4 or the literature [12] may rule out an area such as Alaska or Terra del Fuego, or suggest regions for solar cell collectors (the Sahara, Arizona, etc.), but local information is required for actual system and device design.

Other factors that must be considered are altitude and the nature of the local horizon. Perhaps the most important effect in urban areas is shadowing from local structures. Consider, for example, the fact that the net sea level solar energy input to the earth is 3,770 Q each year (ignoring clouds). If we return to Figure II.5 and compute the insolation predicted for an earth completely covered with ideal two-axis tracking collectors, the calculated value for insolation is 6,160 Q annually. The difference between this value and the 3,770 Q actually annually available lies in the fact that in the case of an earth totally covered with collectors, the collectors would, in part, shadow each other, reducing the insolation to the actually available value. The use of tracking collectors cannot increase the total amount of insolation available, but they do allow an increase in the energy density of the collected energy. For example, the 3,770 Q that does reach the earth's surface each year corresponds to an average energy density of 2,120 kwh/m^2 per year for unshadowed collectors. Thus, the net effect of tracking collectors is to reduce the total collector area required to provide a given amount of energy.

Table II.4

Effective insolation for selected cities with and without weather effects and for tracking two-axis and horizontal, fixed position collectors

Location	Lat (°)	Insolation (kwh/m^2) Maximum Two-axis Collector	Including Weather Two-axis Collector	Fixed Collector
In the United States [11]				
City/State				
Honolulu, HI	21.3	3,610	2,340	1,590
Miami, FL	25.8	3,570	2,320	1,550
New Orleans, LA	30.0	3,550	2,120	1,370
Phoenix, AZ	33.4	3,520	3,020	1,890
Santa Barbara, CA	34.4	3,510	2,530	1,560
Flagstaff, AZ	35.2	3,490	2,510	1,550
Fresno, CA	36.7	3,480	2,850	1,740
Washington, DC	38.9	3,460	2,040	1,210
New York, NY	40.8	3,440	2,060	1,220
Boston, MA	42.2	3,420	1,980	1,150
Burlington, VT	44.5	3,370	1,680	970
Seattle, WA	47.6	3,350	1,570	880
Fairbanks, AK	64.8	3,030	1,450	670
Elsewhere in the world [21-26]				
City/Country				
Athens, Greece	38.0	3,470	2,770	1,920
Mexico City, Mexico	19.2	3,620	2,700	1,870
Port Harcourt, Nigeria	4.9	3,700	2,137	1,444
Jakarta, Indonesia	7.5*	3,670	2,090	1,453
Rio de Janero, Brazil	22.5*	3,600	2,420	1,682
Perth, Australia	32.2*	3,530	2,690	1,905
Wellington, New Zealand	42.0*	3,420	2,740	1,922

* South of the equator

Light Collection

Because of the high degree of purity required of the semiconducting materials used in solar cells, the materials are expensive. The fabrication processes involved in converting the raw semiconductor into solar cells is labor intensive and costly (see Chapters VIII-X). As a result, current solar cell systems cost in excess of $4,000 per peak kilowatt of generating capacity, as opposed to a conventional power plant which costs approximately $1,200 per kilowatt of installed generating capacity. An attractive method of reducing the cost of a solar cell energy system is to substitute less expensive mirrors (or lenses) for solar cells and to use these mirrors (or lenses) to focus sunlight on a relatively small area of solar cells--as depicted in Figure II.6. Besides reducing the overall cost, such a concentration has an additional advantage. Any solar cell has a certain number of ways in which energy can be lost--internal loss mechanisms. In a light concentrating system the higher solar flux saturates many of these loss mechanisms (a topic to be discussed in detail in a later chapter), yielding a higher operating efficiency for the solar cells and for the entire collecting system. However, it is important to note that the performance of any large light concentrating system will depend strongly on the difference in direction between the system normal and the sun. This requirement, implies that the light collecting/concentrating system must be of the tracking type. Thus, any net reduction in overall system cost will depend on both the relative cost of the lenses (or mirrors) and of the solar cells, as well as the expense incurred in providing the tracking mechanism. This section will discuss, briefly, the important optical aspects of light collecting/concentrating systems; leaving until later any interactions between the light and the semiconducting materials.

In general, two types of optical systems are utilized in solar energy collectors with solar cells; lens and mirror systems. Both types of system appear in cylindrical and circular symmetries. The shapes and sizes of the optical components in these solar energy concentrating/collecting systems are largely a result of the twin requirements of minimum cost and of large aperture-to-focal-length ratio (i.e., the requirement for a high degree of light concentration).

Lens Systems

Two types of lenses are commonly employed in solar cell concentrating systems, the so-called standard lens, as depicted in Figure

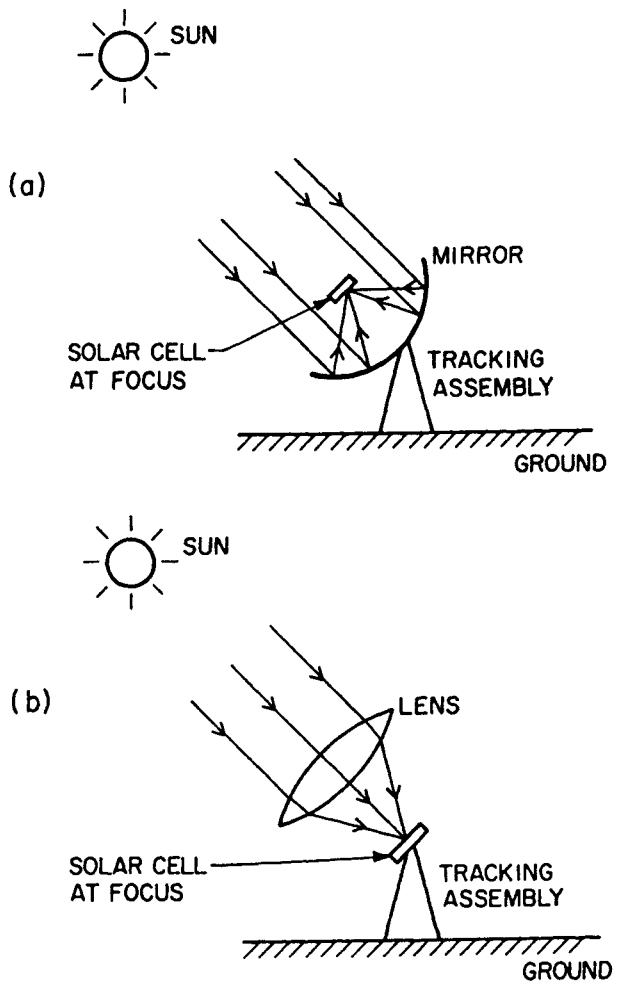

Figure II.6. Techniques for concentrating sunlight on a solar cell.

II.7a, and the Fresnel lens, as shown in Figure II.7b. The Fresnel lens is generally favored because it is thinner and uses far less material, resulting in reduced weight and cost.

Optically, the Fresnel lens is a close equivalent to the thin, conventional lens exemplified by Figure II.7a. (A thin lens is any lens in which the thickness of the lens is small compared to the focal length, F, of the system.) The focal length of a thin lens, with one plane surface is given by:

$$F = R/(n - 1), \qquad (II.9)$$

where n is the index of refraction of the material from which the lens is constructed and R is the radius of curvature of the curved surface.

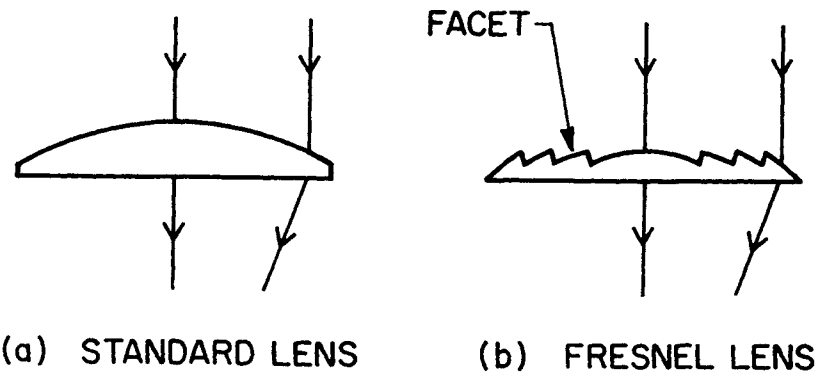

Figure II.7. A standard plano-convex lens and the equivalent Fresnel lens. At the same radial displacement, both lens types induce the same deviation of the incoming solar rays.

As evident in Figure II.7b, in a Fresnel lens, the smooth, even curvature of the standard lens surface is replaced by a number of thin, concentric rings, or facets, with flat surfaces. Each facet is set at the correct angle to refract incoming light rays to the focus*. The discrete facet steps introduce some error into the precision of the focus and some light is lost upon scattering from the vertical faces of the facet steps. Even though the "picture" at the focus is highly distorted by a Fresnel lens, it is still important that any system with a Fresnel lens as the focusing device, track the sun. Light rays entering the system, not parallel to the optic axis have different focal lengths from those entering parallel to the optic axis. The result of failure to accurately track the sun is an increasingly hazy image and a rapid decrease in the collectable optical energy density. Exact corrections for the focal location may be found in the literature [27, 28].

* Such a lens, whether it is in a circular or in a cylindrical symmetry, as in Figure II.8, has a focal length as given by Equation II.9.

Mirrors

The simplest form of mirror system is a flat, reflecting surface with a light path as shown in Figure II.9a. A light-collecting system using a plane mirror implies that the mirror has the same size of area as the solar cell, since no focusing effect is present. Light concentration can be achieved by using several mirrors aligned at specified angles as shown in Figure II.9b. Tracking devices for each mirror are clearly required in order to follow the sun during its daily motion.

A system utilizing two plane mirrors to focus light on a photo-

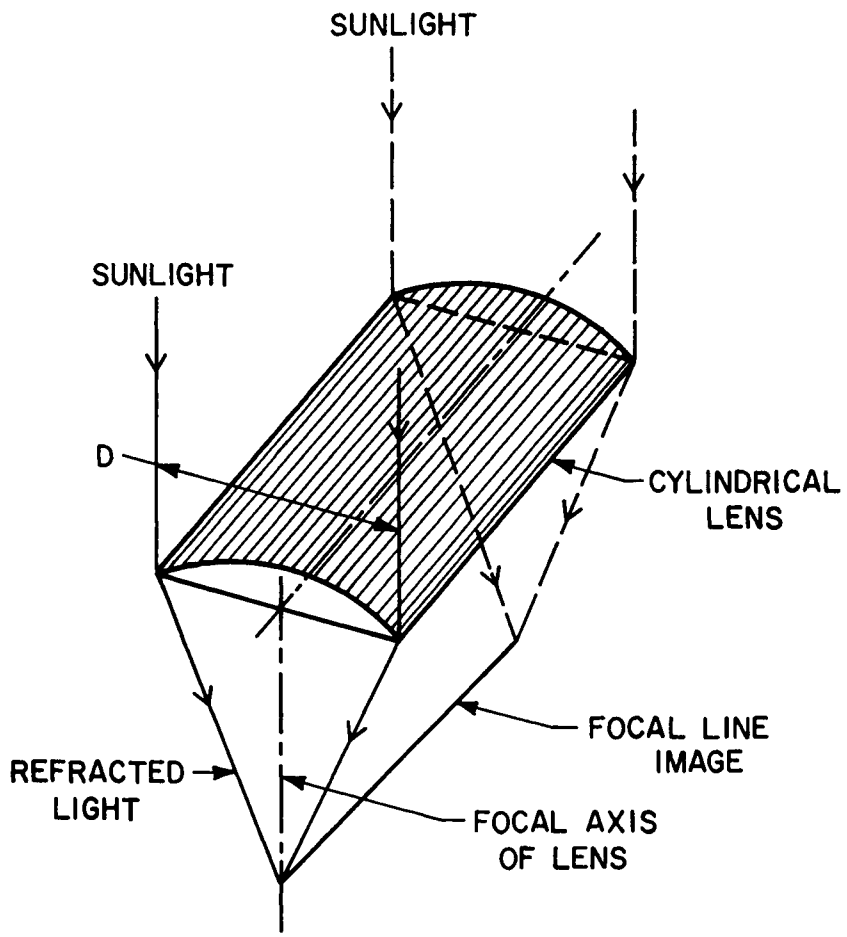

Figure II.8. A diagram of a cylindrical configuration of a Fresnel lens.

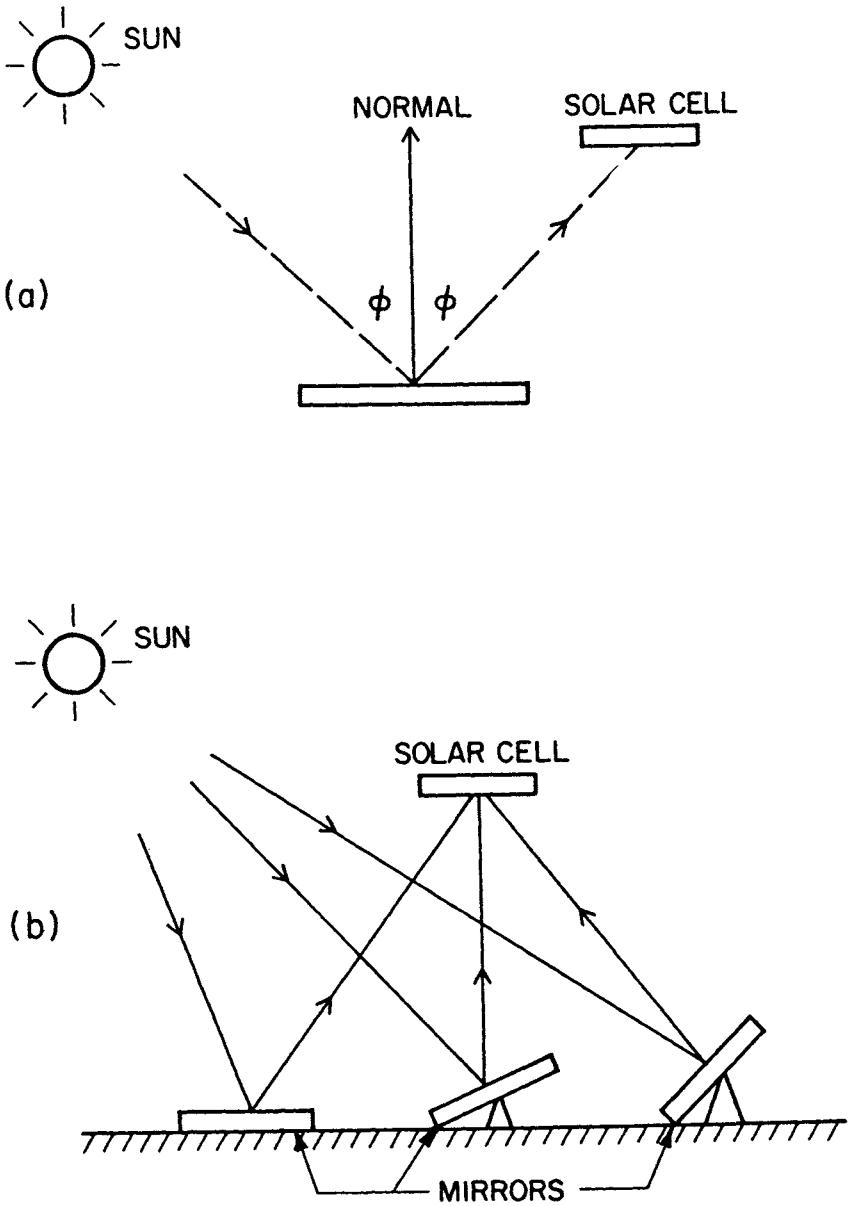

Figure II.9. Simple mirror systems for use in connection with solar cells: (a) a single mirror and (b) a system of mirrors.

voltaic energy converter (solar cell) is depicted in Figure II.10. Note that such a system does not trap all of the incoming light, and that it requires a very deep and, therefore, large area mirror. This system could be

converted to conical symmetry by rotation about the central axis. Combinations of plane mirrors with Fresnel lenses, to provide a focusing effect, are also possible [29].

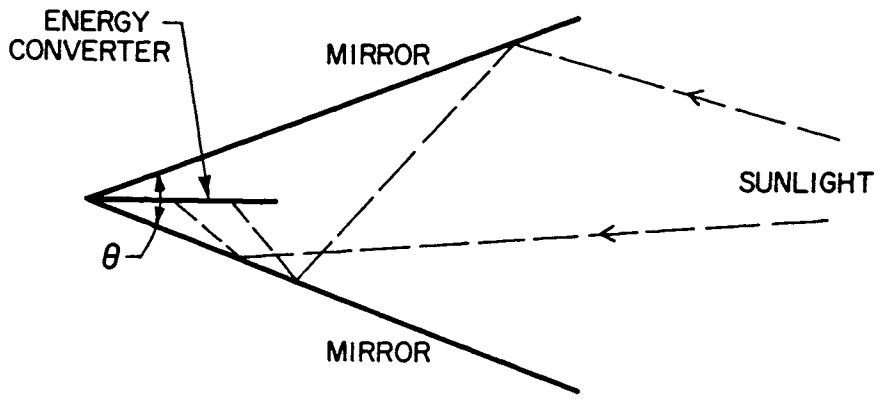

Figure II.10. A deep two mirror focusing system.

The mirrors employed do not have to be of the plane type. An optical diagram for a curved spherical symmetry mirror is displayed in Figure II.11. In this figure, consider an incoming ray of light, at a height, h, above the center of curvature. This ray of light reflects off the mirror

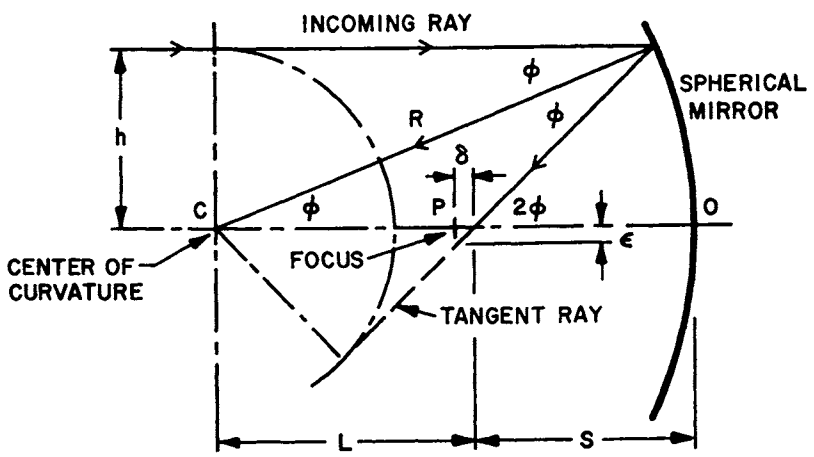

Figure II.11. A basic spherical mirror. P denotes the paraxial focus position. Note that L is always greater than S.

surface and passes close to the focus point, P. The nominal focal length, S, is given by:

$$S = R(2 - 1/\cos\phi), \tag{II.10}$$

where:

$$\phi = \text{arc } \sin\{h/R\}. \tag{II.11}$$

The intercept of the reflected ray, S, with the center line, CPO, is the small distance, δ, from the point of focus, P. This distance is called the longitudinal spherical aberration. The lateral spherical aberration is ϵ; h is the vertical distance from P to the light ray at a distance, S, from the mirror center, O. Clearly, both the longitudinal and lateral spherical aberrations are a function of the ray height, h. Thus, the use of a spherical mirror leads to a "fuzzy" focus. This requires that the energy converting device, which is to be placed at the focus of the mirror, must be carefully shaped to maximize the collection of light and the conversion of the light energy.

In the upper portion of Figure II.12, the outline of a parabolic mirror is displayed. The mathematical description of the mirror surface is:

$$x = (1/4S)y^2. \tag{II.12}$$

The focus of a parabolic mirror is sharp for all light rays entering parallel to the optic axis. However, the focus point will shift if the incoming light rays are not parallel to the optic axis. The end result is an ellipsoidal focal volume, as depicted in the lower portion of Figure II.12. This is a powerful argument for tracking mirrors because tracking will keep the incoming light rays as close to parallel to the optic axis as possible and so maintain a sharp focus.

In considering solar cell energy light converting/collecting systems, there are three basic configurations of parabolic mirrors [30]. These are displayed in Figure II.13. The initial case, (a), is a parabolic mirror facing the sun and focused on a photovoltaic energy converter which has its back towards the sun. The light concentration for this example is nine to one, since the back of the converter is considered to be nonconverting. Case (b) in Figure II.13 folds the energy converter, so that both sides are capable of converting sunlight to electrical energy, and places the

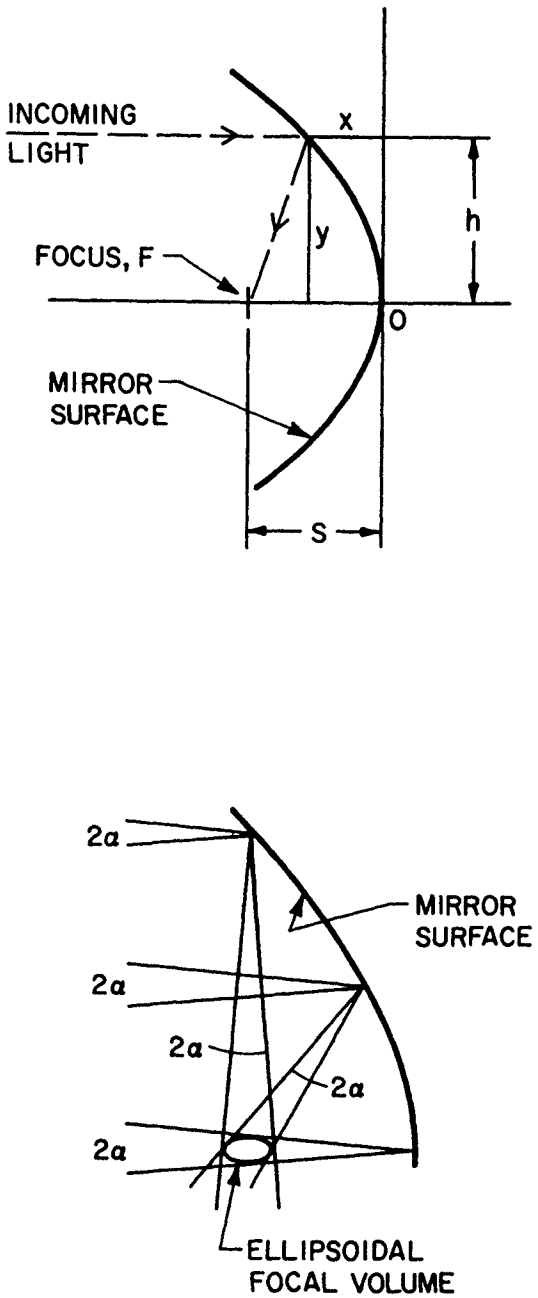

Figure II.12. Parabolic mirror configurations. The lower figure demonstrates the change in focus with mirror-to-light source orientation.

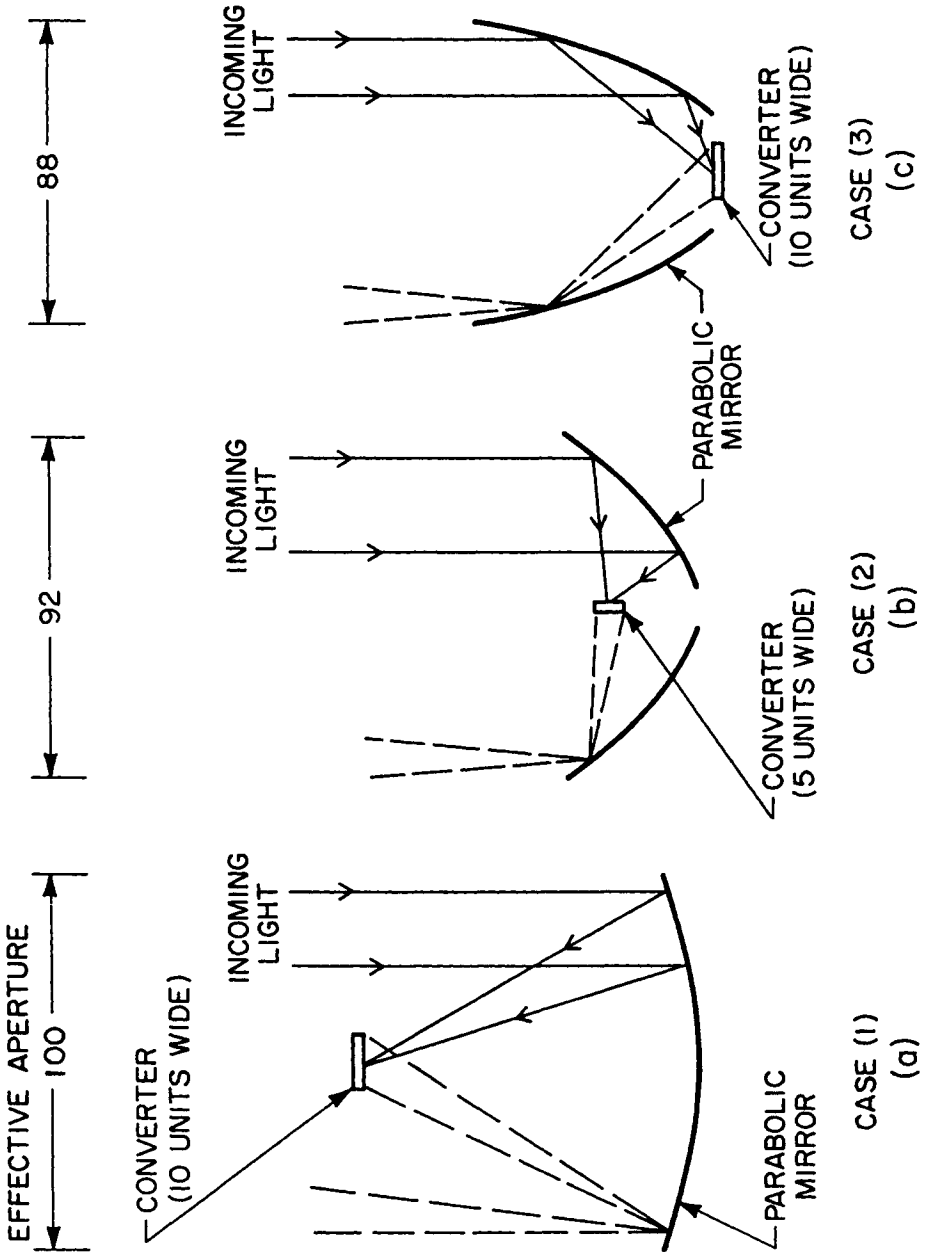

Figure II.13. Three types of parabolic focusing mirror systems for use with solar energy converters [after 30].

converter parallel to the original light ray direction. Here, the optical concentration is also approximately nine to one, owing to some non-reflecting areas along the central axis. The final case, (c), has both the converter and a very deep mirror facing the sun. This configuration utilizes more of its mirrors, but the effective optical concentration is smaller than the other two options. The principal advantage of this variety of mirror/solar cell lies in the fact that the solar cells are close to the ground and mechanical cooling is more easily effected.

There are many other types of lens and mirror energy collection systems which have been proposed over the years, both for fixed and for tracking systems. For a more detailed presentation, the reader is referred to Meinel [31].

Optical Materials

Before leaving light-collecting systems, we should discuss one additional feature of these systems; the nature of the materials through which the light must pass (in a lens system) or off which it must reflect (in a mirrored system). In all cases, we need to strive for minimum cost and maximum performance, while maintaining both initial surface accuracy and maximizing the life expectancy of the optical surfaces involved. The life expectancy is a vital factor as the solar collector is mounted out-of-doors and will be subjected to weather, temperature variations and sunlight for many years.

Consider possible materials for constructing lenses. Generally, we are limited to quartz, glass or plastics. Quartz passes light of a wide range of wavelengths, becoming opaque only for wavelengths less than 0.12 microns. From Figure II.1, we see that the solar output for wavelengths less than this number is effectively zero. However, quartz is expensive and, therefore, is not an economically wise choice. Glass is also transparent over a wide range of wavelengths, being opaque only for ultraviolet wavelengths less than 0.38 microns and for selected spectral regions in the infrared. Study of Figure II.1 indicates that the amount of energy contained in these regions of the solar spectrum is small at the earth's surface (approximately 8% of the total). It will be shown in subsequent chapters that, owing to the nature of the materials normally used in solar cells, infrared light of wavelengths longer than 1.2 microns is relatively unimportant. Thus glass, which is inexpensive, easily cast into optically desirable shapes is an excellent possibility even though it is somewhat heavy.

There is a wide variety of plastic materials from which lenses (standard or Fresnel) can be constructed, including vinyl, polyethylene, etc. Plastics can be tailored to provide efficient light transmission in desired wavelengths with low reflection. The desirable property which is most difficult to obtain in plastics is durability when exposed to sunlight and various weathering elements. However, like glass, plastics can be cast into desired shapes, and, unlike glass, plastics are lightweight.

Besides the transmission of light through a lens, we must consider the phenomenon of reflection of light from the surfaces of the lens. Consider the case for light traveling through a medium with an index of refraction, n_1, and an extinction coefficient, k_1. The photons, which make up this light, impact a lens material with an index of refraction, n_2, and extinction coefficient, k_2, at an angle, θ, to the lens normal. The fraction, f, of the light which is reflected from the lens/medium interface is given by:

$$f = [(n_2 - n_1)^2 + (k_2 + k_1)^2]/[(n_2 + n_1)^2 + (k_2 + k_1)^2], \qquad \text{(II.13)}$$

where the index of refraction and the extinction coefficient of a material are related to the permittivity of the material, ϵ, the conductivity of the material, σ, and the frequency, υ, of the photons by:

$$\epsilon = n^2 - k^2 ,$$

and (II.14)

$$2nk = \sigma/(2\pi\upsilon\epsilon).$$

Note that the index of refraction for air (or for a vacuum) is unity and that the extinction coefficient for both vacuum and air is zero. Using this fact, together with Equation II.13, it is possible to determine the fraction of energy reflected as a function of the index of refraction of a lens material with a close-to-zero extinction coefficient. The results of such a calculation are presented in Table II.5.

Clearly, a low index of refraction material is desirable in a lens system. We can compensate, to some extent, by the use of antireflection coatings--at the cost of added system complexity and expense. (Antireflection coatings of as many as seven layers are employed in high

precision camera lenses. Such a complex process is too expensive to be used in solar cell systems.)

Table II.5

The fraction of light energy reflected as a function of the index of refraction for lenses constructed of low extinction coefficient materials

Index of refraction	1.0	1.25	1.5	2.0	2.5	3.0
Fraction reflected	0.0	0.012	0.04	0.111	0.184	0.444

In the construction of mirrors it is possible to use, as the reflecting surface, a metal such as aluminum or some alloy (e.g., the commercial alloy, Alzak). We can use a sheet of metal, or evaporate a thin reflective surface over some, adequately smooth substrate. This latter technique produces front-surface mirrors and has the disadvantage that the reflecting surface is subject to abrasion and chemical weathering processes; influences that may degrade the reflecting surface within a relatively short time--days, in some instances. To circumvent this problem, we can make use of second-surface mirrors. Here, the reflective layer is placed behind a transmissive material (glass, quartz or some plastic) that acts as the mirror substrate as well as protecting the reflective layer. The disadvantage in this situation arises from transmission losses as light passes through the protecting layer*.

Maximum Optical Concentration

After considering aberration effects and the problems inherent in the construction of large lens (or mirror) light collecting systems, an estimate can be formed of the maximum flux concentration that may reasonably be expected from commercially viable lens and mirror systems. These values are provided in the following table, Table II.6.

As we will observe later, the values for optical concentration in Table II.6 are more than adequate for work with solar cells. A smaller concentration would underuse the cells, a greater would overstress them.

* Note that the light must pass through the transparent layer twice!

Table II.6

Estimated maximum commercially viable light flux concentrating ratios [32]

Type of collecting system	Fresnel Lens	Mirror
Parabolic optics	10 - 30	40 - 60
Circular optics	100 - 400	1400 - 3200

References

1 A. J. Duffle and W. A. Beckman, Solar Energy Thermal Processes, John Wiley and Sons, New York, 1974.
2 M. P. Thakaekara, in Solar Energy, Vol. 14, 1973, p. 3.
3 C. E. Backus, Solar Cells, IEEE Press, New York, 1976, p. 3.
4 M. P. Thakaekara and A . J. Drummond, in Nature of Physical Science, Vol. 229, 1971, p. 6.
5 E. G. Gibson, The Quitet Sun, NASA, Washington, D. C., 1973, Appendix.
6 N. Robinson, Solar Radiation, Elsevier, Amsterdam, 1976.
7 Reference 5, p. 14.
8 E. Petit, in Astrophysics, J. A. Hynek, editor, McGraw-Hill, New York, 1951.
9 The International Symposium on Solar Radiation Simulation, Institute of Enviornmental Sciences, 1965.
10 S. I. Rasool, Physics of the Solar System, NASA, Washington, D. C., 1972.
11 Figures 11.1 - 11.5 and portions of Table II.3 originally appeared in an article by the author entitled, "Solar Energy Collector Orientation and the Tracking Mode", in Solar Energy, Vol. 19, 1971. Table II.4 is derived from an article by the author entitled, "Solar Energy and the Residence: Some Systems Aspects", in Solar Energy, Vol. 19, 1977, p. 589.
12 P. E. Glaser, in Physics Today, Feb. 1977, p. 30.
13 E. G. Laue, in Solar Energy, Vol. 13, 1970, p. 43.

14 A. M. Zarem and D. D. Erway, editors, Introduction to the Utilization of Solar Energy, McGraw-Hill, New York, 1963.
15 J. A. Eddy, in Scientific American, May 1977, p. 80.
16 J. D. Hays, J. Imorie and N. J. Shakleton, in Science, Vol. 194, 1976, p. 1121.
17 J. Ruffner and F. E. Bair, The Weather Almanac, Gale Research, New Jersey, 1974.
18 Climates of the States I and II, U. S. National Oceanic and Atmospheric Administration, Washington, D.C., 1974.
19 F. A. Berry Jr., E. Bullay, N. R. Beers, Handbook of Meterology, McGraw-Hill, New York, 1975, p. 988-995.
20 H. McKinley and C. Liston, The Weather Handbook, Conway Research, 1974.
21 G. L. Morrison and Sudjito, in Solar Energy, Vol. 49, 1992, p. 65.
22 A. Kuye and S. S. Jagtap, in Solar Energy, Vol. 49, 1992, p. 139.
23 M. Nunez, in Solar Energy, Vol. 44, 1990, p. 343.
24 B. E. Western, in Solar Energy, Vol. 45, 1990, p. 14.
25 E. S. C. Cavalcanti, in Solar Energy, Vol. 47, 1991, p. 231.
26 World Weather Records, U. S. National Oceanic and Atmospheric Administration, Washington, D. C., 1987, Vol. I and II.
27 A. B. Meinel and M. F. Meinel, Applied Solar Energy, An Inroduction, Addison-Wesley, Reading, Massachussets, 1976, p. 146-147.
28 Reference # 27, p. 144-145 and 148-149.
29 R. R. Aoarisi, Y. G. Kolos and N. I. Shatof, Semiconductor Solar Energy Converters, V. A. Barn, editor, Translation Consultant's Bureau, New York, 1989, p. 10.
30 V. B. Veinberg, Optics in Equipment for Utilization of Solar Energy, State Publishing House, Moscow, 1959, p. 100.
31 Reference # 27, Chap. 27.
32 Reference # 27, p. 172.